sity of Coimbra. The other (PAT), acknowledges the financial support of the SERC.

References

ABDULLAEV, A. A., VASIL'EVA, A. V., DOBRZHAUSKIĬ, G. F. & POLIVANOV, Y. N. (1977). *Sov. J. Quantum Electron.* **7**(1), 56–59.
ABRAHAMS, S. C., BERNSTEIN, J. & LIMINGA, R. (1980). *J. Chem. Phys.* **72**(11), 5857–5862.
BURKOV, V. J., KIZEL, V. A., PEREKALINA, Z. B., KOZLOVA, N. L. & SEMIN, G. S. (1973). *Sov. Phys. Crystallogr.* **18**(2), 196–197.
DEVARAJAN, V. & GLAZER, A. M. (1986). *Acta Cryst.* A**42**, 560–569.
GALLAGHER, P. K., ABRAHAMS, S. C., WOOD, D. L., SCHREY, F. & LIMINGA, R. (1981). *J. Chem. Phys.* **75**, 1903–1906.
GLADKII, V. V. & ZHELUDEV, I. S. (1965). *Sov. Phys. Crystallogr.* **10**, 50–52.
GLAZER, A. M. & STADNICKA, K. (1986). *J. Appl. Cryst.* **19**, 108–122.
HAUSSÜHL, S. (1978). *Acta Cryst.* A**34**, 547–550.
HIROTSU, S., YANAGI, T. & SAWADA, S. (1968). *J. Phys. Soc. Jpn,* **25**(3), 799–807.
International Tables for X-ray Crystallography (1974). Vol. IV. Birmingham: Kynoch Press. (Present distributor Kluwer Academic Publishers, Dordrecht.)
LIMINGA, R., ABRAHAMS, S. C. & BERNSTEIN, J. L. (1980). *J. Appl. Cryst.* **13**, 516–520.
PAULING, L. (1927). *Proc. R. Soc. London Ser. A,* **114**, 181–211.
POHL, D. (1978). *Acta Cryst.* A**34**, 574–578.
RAMACHANDRAN, G. N. (1951). *Proc. Indian Acad. Sci.* **33**, 217–227.
STADNICKA, K., GLAZER, A. M. & KORALEWSKI, M. (1987). *Acta Cryst.* B**43**, 319–325.
STADNICKA, K., GLAZER, A. M. & MOXON, J. R. L. (1985). *J. Appl. Cryst.* **18**, 237–240.
TESSMAN, J. R., KATTA, A. H. & SHOCKLEY, W. (1953). *Phys. Rev.* **92**, 890–895.
THOMAS, P. A. (1988). *J. Phys. C,* **21**, 4611–4627.
ZACHARIASEN, W. H. (1967). *Acta Cryst.* **23**, 558–564.

Acta Cryst. (1989). B**45**, 355–359

Single-Crystal X-ray Study of the Decagonal Phase of the System Al–Mn

BY W. STEURER

Institut für Kristallographie und Mineralogie der Universität, Theresienstrasse 41, *D*-8000 *München* 2, *Federal Republic of Germany*

AND J. MAYER†

Institute für Physik, Max-Planck-Institut für Metallforschung, Heisenbergstrasse 1, *D*-7000 *Stuttgart* 80, *Federal Republic of Germany*

(*Received* 17 *July* 1988; *accepted* 16 *March* 1989)

Abstract

A single crystal of the metastable decagonal phase of the system Al–Mn with the composition $Al_{0.78(2)}Mn_{0.22(2)}$ and approximate dimensions $0.25 \times 0.13 \times 0.08\,mm^3$ has been investigated by various X-ray film methods and on a four-circle diffractometer. The diffraction pattern can be indexed using four reciprocal lattice vectors pointing to the vertices of a pentagon $a_1^* = a_2^* = a_3^* = a_4^* = 0.2556\ (1)\ Å^{-1}$ and one normal to them parallel to the tenfold axis $a_5^* = 0.08065\ (5)\ Å^{-1}$ [$a_5 = 12.400\ (7)$ Å]. The X-ray photographs indicate that this two-dimensionally quasicrystalline phase is highly ordered. Nevertheless, a considerable amount of diffuse scattering is observed in the reciprocal lattice layers perpendicular to the tenfold axis.

Introduction

Since the discovery of the first quasicrystalline phase, which was icosahedral (Shechtman, Blech, Gratias & Cahn, 1984), numerous new quasicrystals have been detected, some of which have one-dimensional lattice periodicity. In a few cases the point symmetry of these two-dimensional quasicrystals has been found to be octagonal or dodecagonal (Kuo, 1987*a*). Mostly, however, they show decagonal symmetry. Such phases have been prepared in the systems Al–Mn, Al–Fe, Al–Ru, Al–Pt, Al–Pd, Al–Cr(Si), Al–Co, Al–Ni(Si), Al–Rh and Al–Os (Kuo, 1987*b*). With the exception of the icosahedral phase of the system Al–Li–Cu (Mai, Zhang, Hui, Huang & Chen, 1987; van Smaalen, Bronsveld & de Boer, 1987) all single-crystal diffraction studies of quasicrystals have been performed by electron scattering because of the lack of large single crystals. Since the electrons have a very short wavelength, leading to a large radius of the Ewald sphere and also a stronger interaction with matter than X-rays, an interpretation of the diffraction patterns in terms of a simple kinematical approach and thus a quantitative structure determination is in most of the cases not possible. Furthermore, surface effects and structural changes during specimen preparation might obscure the bulk information.

† Present address: Materials Department, College of Engineering, University of California, Santa Barbara, CA 93106, USA.

0108-7681/89/040355-05$03.00

The aim of the present study was, preceding a quantitative structure determination, to analyse the X-ray diffraction patterns for diffuse scattering, as well as performing the usual inspection of Bragg reflections. From this, it is possible to obtain an idea of the degree of order and disorder in this quasicrystalline structure.

Experimental

Al–14at.%Mn alloys were prepared from 99·99% (Al) and 99·9% (Mn) pure starting materials. Rods about 1 cm in diameter and 10 cm long were obtained by pouring the melt into a water-cooled copper mould. The alloys contain a dense packing of decagonal-phase precipitates, with mean dimensions of around 0·2 mm, embedded in an Al-rich matrix. A microprobe analysis of the precipitates showed that the Mn content is 22 (2)at.%.

To isolate the decagonal-phase precipitates, 0·5 mm slices were cut and the Al matrix removed by electrochemical etching in a solution of 2% KI in methyl alcohol. A voltage of 10 V was applied using platinum electrodes. In this way the matrix can be completely removed while virtually no etching of the decagonal phase is observed. In this state the precipitates are still connected to each other by the intergrowth of the dendritic arms of the crystals. Single crystals have to be extracted by carefully crushing this texture under a light microscope. Typical crystals obtained by this method have dimensions of about 0·001 mm^3. The crystal was mounted on the top of a glass capillary and aligned using the precession method. The precession and cone-axis X-ray photographs were recorded using a 12 kW rotating-anode assembly (Rigaku RU-200) with an Mo anode and a Ge(111)–Johansson-type monochromator. The exposure times were about one week for each photograph. The Laue photographs were taken on the same equipment but without the monochromator.

Following the film investigations the crystal was removed from the capillary and mounted with its unique periodic axis parallel to the capillary to optimize the conditions for data collection on the four-circle diffractometer (Enraf–Nonius CAD-4). The reciprocal-lattice basis vectors were refined from 25 reflections.

Results and discussion

A first glance at the precession and cone-axis photographs shows that the diffracted X-ray intensity is mainly concentrated in the Bragg reflections. All photographs exhibit reflections which are elongated circularly but sharp radially. Since the photographs are taken along various directions, *i.e.* the tenfold (10), pseudo-fivefold (ps5), pseudo-threefold (ps3) and twofold (2) axes (*cf.* Fig. 1), it follows that the Bragg reflections are shaped like small spherical shell segments. The dimensions of these segments do not vary significantly with position in reciprocal space. This would be the case if the broadening of the reflections was caused by a large mosaic spread. Using the same argument, the existence of some intergrown crystal individuals tilted slightly against each other can be excluded. A possible explanation, however, could be that the coherently scattering regions in the crystal are cylindrical domains pointing approximately to the vertices of an icosahedron.

The intensities of the Bragg reflections show a similar decay to those of the comparable periodic phases with increasing scattering angle. This means that the static/dynamic displacements from the mean lattice sites are of the same order as usual and models can be excluded which state that the quasicrystalline structure and symmetry are realized in a statistical way only, *i.e.* by averaging over a structure with large shifts of the atoms from the mean positions.

Indexing

The zero-layer precession photograph with symmetry 10*mm* (Fig. 2*b*) contains the information of the quasicrystal structure projected down [00001] and it might be interesting to compare it with the calculated diffraction pattern of two-dimensional Penrose tiling. Using the structure-factor formula given by Janssen (1986) and an artificial atomic scattering factor the intensities for the reflections with $-3 \leq h,k,l,m \leq 3$ have been calculated and all with $I > 0{\cdot}01 I_{0000}$ plotted (Fig. 2*a*). The best agreement between both patterns is obtained choosing the length of a_i^* to be 0·2556 Å^{-1}.

There is no way of uniquely indexing the diffraction pattern of the decagonal phase. There always remains an ambiguity in the length of the basis vectors of the decagonal reciprocal lattice planes by multiples of $\tau = (5^{1/2} + 1)/2$.

Symmetry

The symmetry of the decagonal phase has been shown to be 10/*m* or 10/*mmm* (Bendersky, 1985) and has recently been studied extensively by electron diffraction (Mayer, 1988). The latter studies indicate that the orientations of the pseudo-threefold and

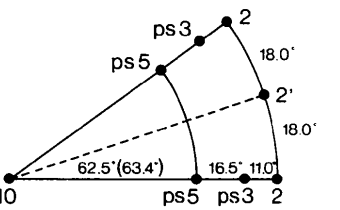

Fig. 1. Schematic representation of the angles between the *n*-fold axes of the decagonal phase. The value for the icosahedral quasicrystal is given in parentheses.

pseudo-fivefold axes of the decagonal phase are in close but not exact metric relationship with the orientations of the corresponding axes in the icosahedral phase of Al–Mn (*cf.* Fig. 1). The recording geometry in the case of electron diffraction is very different from that of the precession method but the result is similar. The electron diffraction pattern corresponds to a zero-layer X-ray precession photograph. However, only in the second case do we get information about the bulk crystal.

Precession photographs correspond to sections of the reciprocal lattice, cone-axis and Laue photographs give gapless information of volumes of reciprocal space. This might be important for detecting and analyzing diffuse diffraction phenomena.

The two-dimensional decagonal symmetry 10*mm* suggested by Mayer (1988) is confirmed by all of the X-ray photographs (Figs. 2–4). As well as the Bragg reflections, the diffuse streaks obey the three-dimensional Laue class 10/*mmm*. From the zero-layer precession photograph (Fig. 2*e*) the pseudosymmetry corresponding to the fivefold axis in the icosahedral case is easily seen. Both the intensity distribution of the Bragg reflections and the direction of the diffuse streaks indicate the violation of the fivefold symmetry. Even

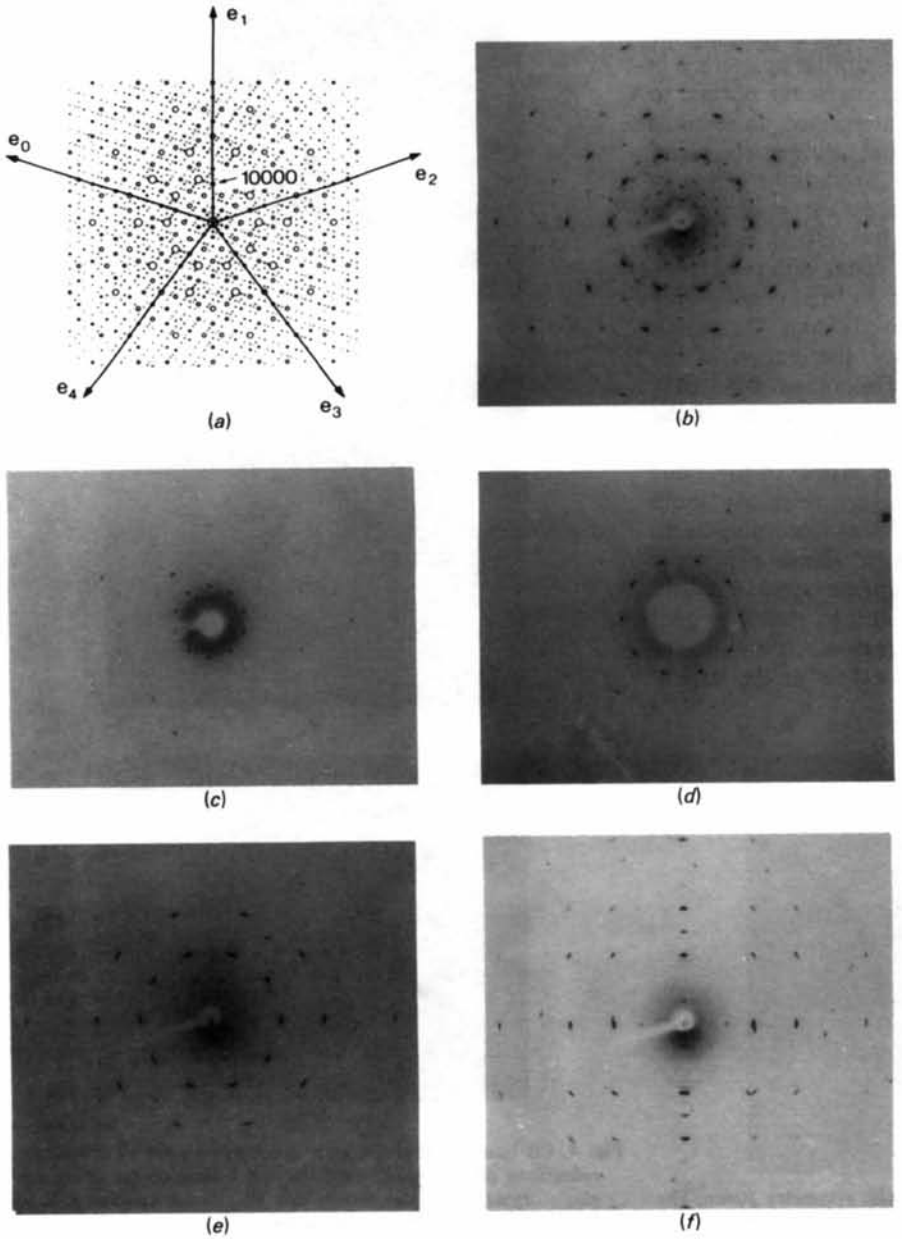

Fig. 2. (*a*) Calculated diffraction pattern of the Penrose tiling. The size of the circles is proportional to the intensities of the reflections. (*b*) Zero-layer precession photograph ($\mu = 30°$) with symmetry 10*mm*. (*c*) First-layer precession photograph ($\mu = 25°$) with symmetry 10*mm*. Note the diffuse ring around the center. (*d*) Second-layer precession photograph ($\mu = 25°$) with symmetry 10*mm*. Note the diffuse ring around the center. (*e*) Zero-layer precession photograph ($\mu = 30°$) with pseudosymmetry 5. Horizontal diffuse streaks and varying intensities of the smallest ring of reflections breaking fivefold symmetry are clearly visible. (*f*) Zero-layer precession photograph ($\mu = 30°$) with symmetry 2*mm*. Vertically only reflections 0000*n* with *n* even are visible. The split reflection on this axis has the index 00002. Note the difuse streaks normal to the tenfold axis.

more sensitive to the detection of pseudosymmetries is the Laue method (Fig. 4*b*), which indicates that the bulk of the reciprocal space is farther away from fivefold symmetry, as can be seen from the zero layer. The same holds for the ps3 axis.

From the precession photograph containing the tenfold axis (Fig. 2*f*) it can be seen that the reflections $0000n$ with n odd are systematically absent indicating a screw axis 10_5.

It is remarkable that nearly all observable reflections of the first-layer precession photograph (Fig. 2*c*) are along the main axes e_i and those of second layer are on the reflection line in between.

Diffuse scattering

The zero-layer precession photograph containing the tenfold axis (Fig. 2*f*) shows some diffuse scattering in the form of slightly modulated short streaks normal to [00001]. These streaks can be interpreted as sections through annular two-dimensional diffuse intensity distributions which are visible *e.g.* around the center of the first- and second-layer precession photographs (Figs. 2*c–d*). The sharpness of the diffuse scattering parallel to [00001] indicates long-range ordered chains in that direction. Perpendicular to the chains only short-range order can be derived from the single maximum of the diffuse intensity distribution in the layers of the reciprocal lattice. This observation is in good agreement with the growth morphology of the crystals (Mayer & Csanady, in preparation).

Much more diffuse scattering is visible in the Laue photographs (Figs. 4*a–c*), which are relatively more exposed owing to the different X-ray recording technique. The Laue photograph with $10mm$ symmetry (Fig. 4*a*) shows some radial diffuse streaks partly crossing Bragg reflections. The diffuse streak system and the Bragg reflections, however, seem to be independent from each other since their widths normal to the streaks are quite different. If we define net planes $(10\bar{1}0)$ with their zone axis [00001] then 'stacking faults' of these planes can lead to the diffuse streaks observed. The short radial streaks pointing to the origin of the reciprocal lattice visible on the strongly overexposed Laue photograph with symmetry $2mm$ (Fig. 4*c*) can be explained by a high mosaic spread in this direction.

The authors are grateful for the assistance of Mrs M. Rapp in specimen preparation, Mrs A. Schmid in taking

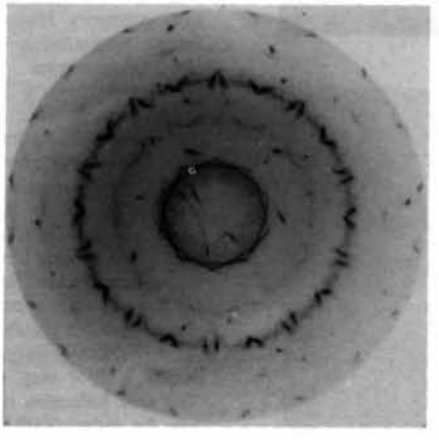

Fig. 3. Cone-axis photograph ($\mu = 30°$) with symmetry $10mm$. The circles correspond to the layers from $-2 \leq n \leq 2$.

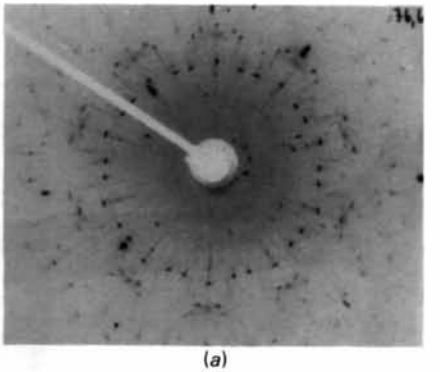

(*a*)

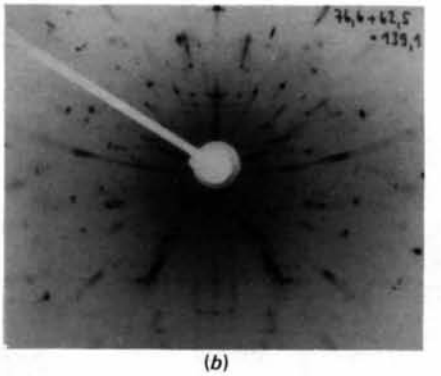

(*b*)

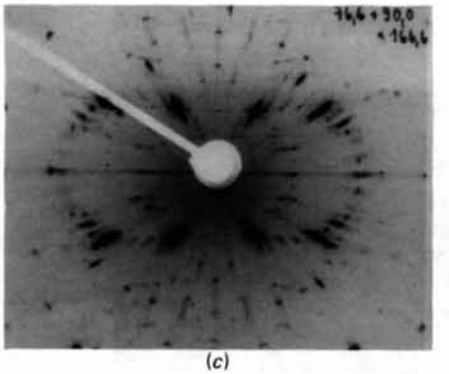

(*c*)

Fig. 4. (*a*) Laue photograph with symmetry $10mm$. A few strong reflections on the photograph do not belong to the decagonal single crystal. (*b*) Laue photograph with pseudosymmetry 5. (*c*) Laue photograph with symmetry $2mm$.

the X-ray photographs and Dr M. Wilkens for stimulating discussions.

References

BENDERSKY, L. (1985). *Phys. Rev. Lett.* **55**, 1461–1463.
JANSSEN, T. (1986). *Acta Cryst.* A**42**, 261–271.
KUO, K. H. (1987*a*). *Acta Cryst.* A**43**, C-312.
KUO, K. H. (1987*b*). *Mater. Sci. Forum*, **22–24**, 131–140.
MAI, Z., ZHANG, B., HUI, M., HUANG, Z. & CHEN, X. (1987). *Mater. Sci. Forum*, **22–24**, 591–600.
MAYER, J. (1988). Thesis, Univ. of Stuttgart, Federal Republic of Germany.
SHECHTMAN, D., BLECH, I., GRATIAS, D. & CAHN, J. W. (1984). *Phys. Rev. Lett.* **53**, 1951–1953.
SMAALEN, S. VAN, BRONSVELD, P. & DE BOER, J. L. (1987). *Solid State Commun.* **63**, 751–755.

Acta Cryst. (1989). B**45**, 359–364

Calculation of the Electron Density Distribution in Silicon by the Density-Functional Method. Comparison with X-ray Results

BY G. J. M. VELDERS AND D. FEIL

Chemical Physics Laboratory, University of Twente, PO Box 217, 7500 *AE Enschede, The Netherlands*

(*Received* 24 *October* 1988; *accepted* 21 *March* 1989)

Abstract

Quantum-chemical density-functional theory (DFT) calculations, using the local-density approximation (LDA), have been performed for hydrogen-bounded silicon clusters to determine the electron density distribution of the Si–Si bond. The density distribution in the bonding region is compared with calculated and X-ray values of the bond in the crystal and found to be in good agreement. Using Hirshfeld's method for charge partitioning, a central Si atom was isolated and used for building a crystal. The corresponding structure factors agree very well ($R \leq 0{\cdot}14\%$) with experimental ones obtained by the *Pendellösung* method.

Introduction

Silicon has been a subject of intensive research for a few decades now but there are still several properties which are not well understood. Theoretical methods, such as band-structure calculations, do not always seem to reproduce experimental results.

Hohenberg & Kohn (1964) have shown that the ground-state electron density distribution $\rho(\mathbf{r})$ fully characterizes all properties of the many-body system in the ground state. As a corollary, no quantum-mechanical method yielding an inaccurate electron density distribution will give proper energy values, unless compensation of errors occurs. With this in mind we set out to calculate the electron density distribution in silicon. This is all the more interesting because the calculations can be compared with the very accurate structure factors of silicon, obtained by Aldred & Hart (1973) and by Saka & Kato (1986) with the *Pendellösung* method. Spackman (1986) has analyzed various sets of measured structure factors and compared them with different theories, while Cummings & Hart (1988) have recently reanalyzed the experiments of Aldred & Hart (1973) making some additional corrections.

The work presented in this paper is based on molecular Hartree–Fock–Slater (HFS) LCAO calculations. The present method cannot handle the periodicity of the crystal. To obtain the density distribution of the silicon crystal, we determined $\rho(\mathbf{r})$ in hydrogen-bounded silicon clusters of increasing size. The larger the cluster, the more a central atom is assumed to resemble the atoms in the crystal. By partitioning the charge distribution in the cluster, a central Si atom can be extracted from the cluster and used for building an infinite crystal by applying the proper symmetry operations.

To verify the assumption and to judge the resulting crystalline electron density distribution, structure factors were calculated and compared with the results of *Pendellösung* measurements by Aldred & Hart (1973) and Saka & Kato (1986), with values recommended by Spackman (1986) on the basis of careful analysis of existing data, and with the outcome of Yin & Cohen's (1982) band-structure calculations.

Computational methods

To calculate the electron density distribution $\rho(\mathbf{r})$ in silicon clusters we employed the HFS-LCAO-DVM version of the LDA method. In the Hohenberg–Kohn–Sham formalism (Hohenberg & Kohn, 1964; Kohn & Sham, 1965) the calculation for spin-restricted states consists of self-consistently solving

$$\left[-\tfrac{1}{2}\nabla^2 + V_{\text{eff}}(\mathbf{r})\right]\varphi_i(\mathbf{r}) = \varepsilon_i\varphi_i(\mathbf{r}) \qquad (1)$$

0108-7681/89/040359-06$03.00